Faraday Discussions

Cite this: *Faraday Discuss.*, 2026, **262**, 515

PAPER

Thermally and base-triggered 'debond-on-demand' crosslinked polyurethane adhesives†

Alarqam Zyaad Tareq, [ab] Matthew Hyder, [a] Josephine L. Harries[c] and Wayne Hayes *[a]

Received 25th April 2025, Accepted 4th June 2025
DOI: 10.1039/d5fd00051c

To address current industrial needs and modern legislation, a series of rapidly degradable and strongly adhering crosslinked polyurethanes featuring the commercially available and degradable chain-extender 2,2′-sulfonyldiethanol have been made for use as depolymerisable coatings and 'debond-on-demand' hot-melt adhesives. Variation of the chain-extended polyurethane (CEPU) composition, through increased hard segment content, provided a route to tailor the mechanical, adhesive, and degradable characteristics, whereby CEPUs with ultimate tensile strengths and elongation at break of up to 42.68 MPa and 17.59 ε, respectively, could be achieved. The adhesive shear strength of the CEPUs was investigated on a selection of substrates with the highest shear strength observed of 7.80 MPa on aluminium. Depolymerization was triggered *via* exposure of the CEPUs to tetrabutylammonium fluoride (TBAF), causing the solubilisation of the CEPUs and the generation of low molecular weight species. Rapid 'debond-on-demand' adhesion was also achieved upon exposure to 1 M $TBAF_{(aq)}$, with losses in shear strength of up to 34% on aluminium when exposed for 30 minutes.

Introduction

Polyurethanes have found wide use in a range of applications including adhesives,[1–3] coatings,[4,5] textiles,[6,7] wearable electronics,[8,9] and biomedical devices,[10,11] to name a few. When compared to their linear counterparts, crosslinked polyurethane possess enhanced mechanical strength, chemical resistance, and heat resistance.[12,13] However, the permanent nature of these covalent crosslinks hinders their ability to be recycled and removed from adhered surfaces, increasing the quantity of materials sent to landfills. With increasing legislative

[a]*Department of Chemistry, University of Reading, Whiteknights, Reading, RG6 6AD, UK. E-mail: w.c.hayes@reading.ac.uk*
[b]*Department of Chemistry, Faculty of Science, University of Zakho, Duhok, 42001, Iraq*
[c]*Domino UK Ltd, Trafalgar Way, Bar Hill, Cambridge CB23 8TU, UK*

† Electronic supplementary information (ESI) available. See DOI: https://doi.org/10.1039/d5fd00051c

and regulatory pressure for recyclable and reusable materials, the ability to remove polymeric materials, such as adhesives, from multicomponent packaging increases their recyclability by eliminating potential contaminants to yield higher quality recycled plastics.

'Debond-on-demand' adhesives are a relatively new class of stimuli responsive polymers (SRPs) which can debond from adhered surfaces upon exposure to specific external physical, biological, or chemical stimuli.[14–17] This phenomenon occurs through stimuli induced changes in their chemical and physical properties at specific locations within their molecular architecture. 'Debond-on-demand' adhesives have been realised through innovative use of supramolecular,[18–22] dynamic covalent bonding,[23–26] vitrimers,[27,28] and self-immolative units.[29–32]

Greenland and co-workers refined their previous fluoride degradable chain-extender system,[29,33] utilised in 'debond-on-demand' adhesives, to afford a tri-armed crosslinker which provided enhanced shear strength and debonding characteristics when compared to the linear counterpart.[34] Recyclable and re-processable epoxy-anhydride based vitrimer adhesives have also been developed based on dynamic transesterification processes to provide repairable characteristics to the materials.[12,35,36] Debondable polyurethane thermoset adhesives reported by Iezzi and co-workers utilised substituted silyl diol chain-extenders, which exhibit on-demand degradation *via* cascading bond cleavage upon exposure to fluoride ions.[35,36] Utilising the dynamic nature of azine functional groups Liu, Li, and co-workers realised a series of dynamic covalent crosslinked polyurethane networks.[37,38] The introduction of azine chain-extenders provided the crosslinked polyurethanes thermal re-processability *via* azine exchange, and acid triggered degradation.[39]

Inspired by the above studies and our realisation of the commercially available 2,2′-sulfonyldiethanol (SDE) as an effective base degradable chain-extender in linear polyurethane 'debond-on-demand' adhesives,[40] herein we report the utilisation of these simple chemistries to the generation of new base susceptible crosslinked polyurethanes for use in depolymerisable coatings and 'debond-on-demand' adhesives.

Results and discussion

The ability to generate 'debond-on-demand' adhesives which possess high shear strength and the ability to rapidly debond from a range of substrates is an attractive material characteristic, especially when those adhesives can be obtained from low cost commercially available starting materials. Having previously established the base susceptibility of the sulfonyl ethyl urethane (SEU) unit to strong bases, namely NaOH, and TBAF,[40] a series of chain-extended crosslinked polyurethane (CEPU) adhesives were synthesised *via* a one-pot two-step method which has previously been deployed to generate analogous recyclable crosslinked polyurethanes,[39] see Scheme 1. Poly(tetrahydrofuran) (PTHF) was chosen as the soft segment for these CEPUs whilst 1,1,1-tris(hydroxymethyl)ethane (TMP) was used to crosslink the synthesised prepolymers. Variations in the hard segment content of the CEPUs (*i.e.* 4,4′-methylenebis(cyclohexyl isocyanate) (HMDI) and SDE molar ratios) were used to tailor the mechanical, adhesive, and degradable characteristics of the crosslinked materials, see Table 1 and ESI, Fig. S1,† for the composition of the CEPUs.

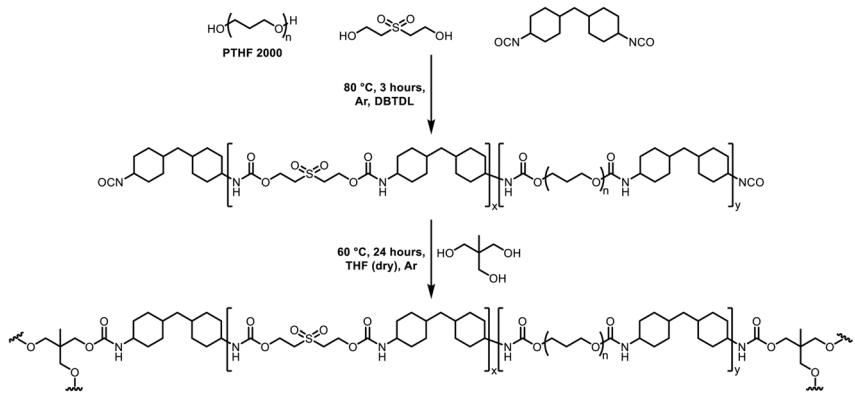

Scheme 1 General synthetic protocol to afford **CEPU1–CEPU4**.

Table 1 Molar ratios of the CEPU compositions and the thermal properties for **CEPU1–CEPU4** (yields are shown in brackets)

CEPUs	PTHF	HMDI	SDE	TMP	T_g (°C)	T_m (°C)	T_{cc}/T_c (°C)
CEPU1 (92%)	1	2.5	0.5	0.667	−77.00[a]	18.84[b], 20.27[c]	−19.06[b], −23.56[c], −26.64[d]
CEPU2 (90%)	1	3	1	0.667	−78.33[a]	54.30[a], 19.03[b], 21.13[c]	−22.60[b], −26.20[c], −28.55[d]
CEPU3 (94%)	1	3.5	1.5	0.667	−78.32[a]	59.57[a], 19.75[b], 1.61[c]	−16.65[b], −20.77[c], −26.38[d]
CEPU4 (95%)	1	4	2	0.667	−78.14[a]	59.34[a], 20.10[b], 21.58[c]	−18.00[b], −23.27[c], −33.12[d]

[a] First heating run 10 °C min^{-1} (isotherm for 60 min at −90 °C). [b] Second heating run 10 °C min^{-1}. [c] Third heating run 10 °C min^{-1}. [d] Second cooling run 10 °C min^{-1}.

The successful synthesis of the CEPUs was confirmed by FT-IR spectroscopic analysis, where the characteristic νN=C=O stretch of the isocyanate at *ca.* 2275 cm^{-1} was not evident, confirming the complete consumption of the isocyanate groups. Furthermore, the presence of absorbance bands at *ca.* 1700–1715 cm^{-1} and *ca.* 3325 cm^{-1} correspond to the νC=O and νN–H stretching vibrations of the urethanes within the polymer backbone, respectively. The additional presence of an absorption band at *ca.* 1320 cm^{-1} confirms the incorporation of the SDE chain-extender. Increases in the hard segment content of the CEPUs increases the intensity of the absorption bands for the urethane and sulfone groups. The FT-IR spectroscopic data of the CEPUs is available in Fig. S2.†

The thermal properties of the crosslinked CEPUs were first investigated *via* thermogravimetric analysis (TGA) to determine their maximum processing temperature, see Fig. 1A and Fig. S3–S6.† As the molar ratio of the hard to soft segments was increased the thermal stability of the CEPUs decreased, whereby the onset of degradation shifted from 254 °C to 233 °C from **CEPU1** to **CEPU4**, most likely attributed to the degradation of the sulfone chain-extender. Additionally, all CEPUs observed complete degradation once the environment reached

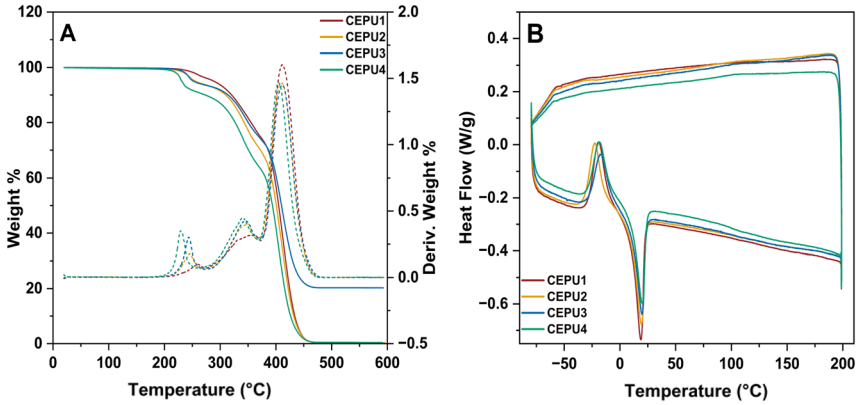

Fig. 1 (A) TGA curves of **CEPU1–CEPU4** from 0 °C to 600 °C at a heating rate of 10 °C min^{-1}, (B) DSC thermograms of the second heating cycle of **CEPU1–CEPU4** from −80 °C to 200 °C at a heating rate of 10 °C min^{-1}.

475 °C. The thermal transitions of the CEPUs were subsequently investigated *via* differential scanning calorimetry (DSC), see Fig. 1B and Fig. S7–S10.† To observe the glass transition temperature (T_g) of the PTHF backbone at *ca.* −78 °C,[41,42] the CEPUs were held at −90 °C for 60 min prior to heating. **CEPU2–CEPU4** exhibit a broad weak melt transition (T_m) around 59 °C, corresponding to the hard domains within the polymer. The associated enthalpy values exhibit a notable increase, ranging from *ca.* 0.03 to 0.64 J g^{-1}, correlating with the increasing content of the hard domains for **CEPU1** and **CEPU4**, respectively. All CEPUs exhibit strong cold crystallization (T_{cc}) and T_m transitions during subsequent heating cycles whereby increases in the hard segment content resulted in slight increases in the T_m, 18.84 °C to 20.10 °C for **CEPU1** and **CEPU4**, respectively.

The temperature dependent viscoelastic properties of the CEPUs were investigated using rheological analysis from 0 °C to 180 °C at a heating rate of

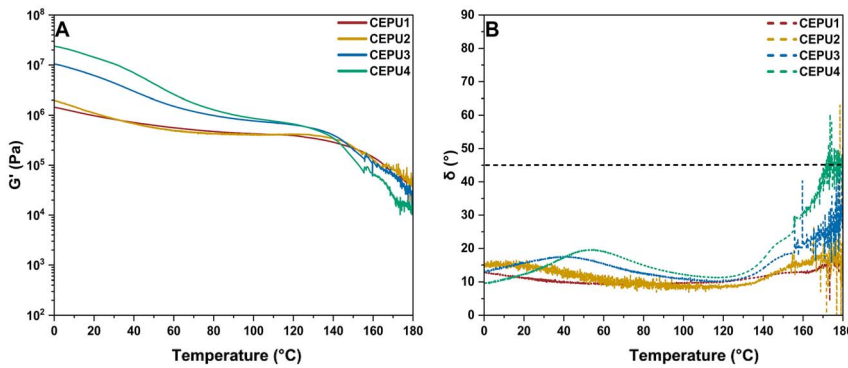

Fig. 2 The rheological behaviour of **CEPU1–CEPU4** over a temperature regime of 0 °C to 180 °C, using a normal force of 1 N and a frequency of 1 Hz. (A) Storage modulus (G') against temperature, (B) phase angle (δ) against temperature, dashed line represents phase transition from viscoelastic solid to viscous liquid.

2 °C min^{-1}, see Fig. 2 and Fig. S11.† Increasing the hard segment content of the CEPUs enhances the initial storage modulus (G') of the materials from *ca.* 1.4 × 10^6 Pa to 2.3 × 10^7 Pa, **CEPU1** and **CEPU4**, respectively. Extended rubbery behaviours up to 120 °C were noticed, and the storage modulus values remained essentially constant around 10^6 Pa, and there was no noticeable microphase separation[39] as a result of the low hard domains content of **CEPU1** and **CEPU2.** Low temperature relaxations were observed for CEPUs with higher hard segment content, corresponding to the melt and reordering of the hard segments within the crosslinked CEPU matrix, consistent with the T_m's from the first heating cycle.

To aid in the investigation of the thermal susceptibility on the bulk morphology of the CEPUs, variable temperature (VT) small angle X-ray scattering (SAXS) and wide angle X-ray scattering (WAXS) experiments were performed on thin film samples of the CEPUs from 25 °C to 200 °C, at 25 °C intervals. At 25 °C the CEPUs exhibit broad Bragg peaks in the SAXS data, increasing the hard domain content from **CEPU1** to **CEPU4** increases the degree and size of the phase separation shifting the q_{max} from 0.52 nm^{-1} to 2.99 nm^{-1}, corresponding to *d*-spacings of 11.99 nm and 2.09 nm, respectively, see Fig. S12 and Table S1.† Two significant peaks were observed in the WAXS diffraction patterns, a sharp peak at 3.7 nm^{-1} (*d*-spacing of 1.69 nm) and broad diffraction peak at approximately 12.6 nm^{-1} (*d*-spacing of 0.49 nm), attributed to the hard segment assembly and hydrogen bonding urethane residues, respectively.[3,43–45] These peaks were used to evaluate the intensity changes of the **CEPU1–CEPU4**, that are directly

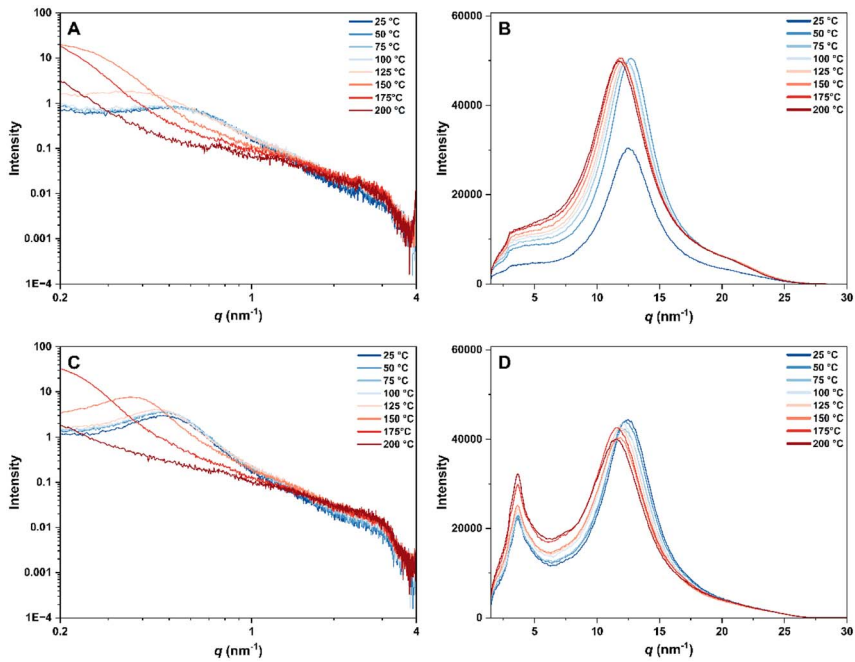

Fig. 3 VT-SAXS and VT-WAXS of **CEPU1** (A and B) and **CEPU4** (C and D) profiles as a function of temperature, recorded at 25 °C intervals from 25 °C to 200 °C at a heating rate of 25 °C min^{-1}.

proportional to the hard segment content. The microphase separated morphologies of the CEPUs were observed to be susceptible to increases in temperature whereby upon heating above 100 °C (**CEPU1** and **CEPU2**) or 125 °C (**CEPU3** and **CEPU4**) the diffraction peak in the SAXS spectra shifted to lower q values before a transition to an amorphous material was evident by the loss of the diffraction peak, see Fig. 3, and Fig. S13.† VT-WAXS of the CEPUs show shifts in the q_{max} of the scattering peak corresponding to a length scale shift from 12.6 nm^{-1} to 11.5 nm^{-1}, this shift is attributed to subtle changes in the hydrogen-bond length between the urethane moieties.[40] Furthermore, the intensity of the diffraction peak at *ca*. 3.7 nm^{-1} increased upon heating corresponding to the change in the polymer structure *via* disassociation between the chains.[46]

Probing the mechanical properties of the CEPUs through tensile stress–strain measurements at a rate of 10 mm min^{-1} illustrated how varying the hard segment composition of the CEPUs affects their unique mechanical properties, see Fig. 4 and Table S2.† Increasing the hard segment content of the CEPUs results in increases in the mechanical properties, *i.e.* the Young's modulus (YM), ultimate tensile strength (UTS), modulus of toughness (MoT), and elongation at break (EB) see *ca*. 1070%, 440%, 1220%, and 200% increases from **CEPU1** to **CEPU4**, respectively, see Fig. 4B–D. Direct comparisons of these degradable CEPUs to those reported within the literature is non-trivial on the account of variations in polymer composition. However, **CEPU1–CEPU4** are compositionally comparable (with exception of the SDE chain-extender) to a series of polyurethanes by Liu, Li,

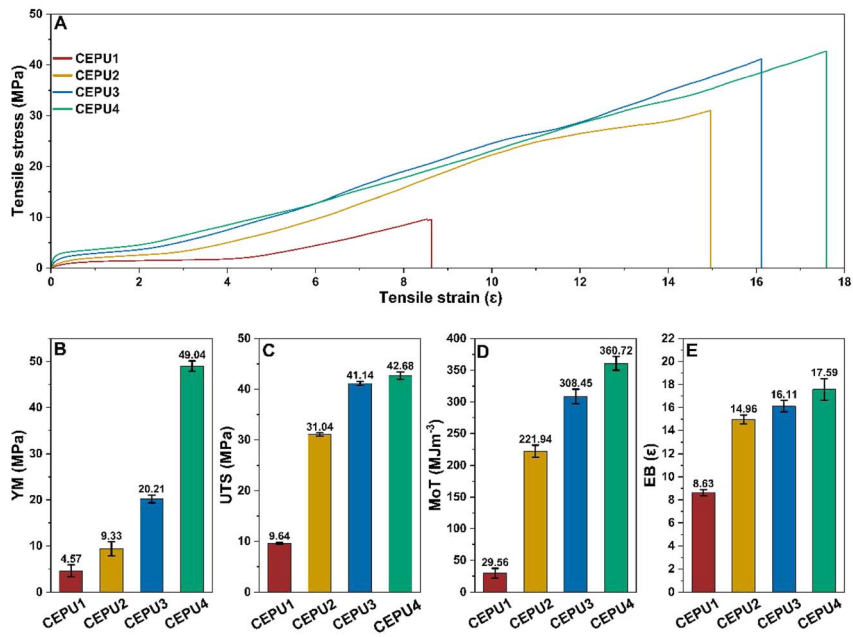

Fig. 4 (A) Representative stress–strain curves of **CEPU1–CEPU4**. (B) Young's modulus (YM), (C) ultimate tensile strength (UTS), (D) modulus of toughness (MoT), and (E) elongation at break (EB) of **CEPU1–CEPU4**. The error shown is the standard deviation between the three repeats for each sample.

and co-workers.[39] Although their FAPUE systems exhibit extraordinary values for YM (up to 225 MPa), at comparable hard segment content **CEPU4** exhibits *ca.* 425% and 300% greater EB and MoT, respectively. An analogous strain hardening profile was observed[5] in the case of supramolecular polyurethane comb elastomers, the non-covalently crosslinked nature of these supramolecular polymers provided comparable EB yet significantly lower UTS when compared to crosslinked **CEPU4**. Further comparisons of the mechanical properties between **CEPU4** and degradable/recyclable crosslinked polyurethanes are provided in Fig. S14.†

The hot-melt adhesive capabilities of the crosslinked CEPUs were investigated using lap shear adhesion tests with glass, aluminium, and Nylon 6,6 substrates. A small disk of polymer (diameter = 4 mm, thickness = 1 mm, and mass = 25 mg) was placed between two substrate coupons and held by clamps on each side with an overlap area of 2.5 cm × 2.5 cm. The CEPUs were adhered at 150 °C for 30 minutes then allowed to cool to room temperature for 30 minutes prior to testing, each sample was tested in triplicate. Increased shear strength was observed for all three substrates as the hard content in the CEPUs was increased from **CEPU1** to **CEPU4**, with up to 258% increase in shear strength, see Fig. 5A–C and Table S3.† To investigate the reusability of these CEPUs as adhesives, the re-adhesion of **CEPU1–CEPU4** over five re-adhesion cycles was subsequently conducted on all

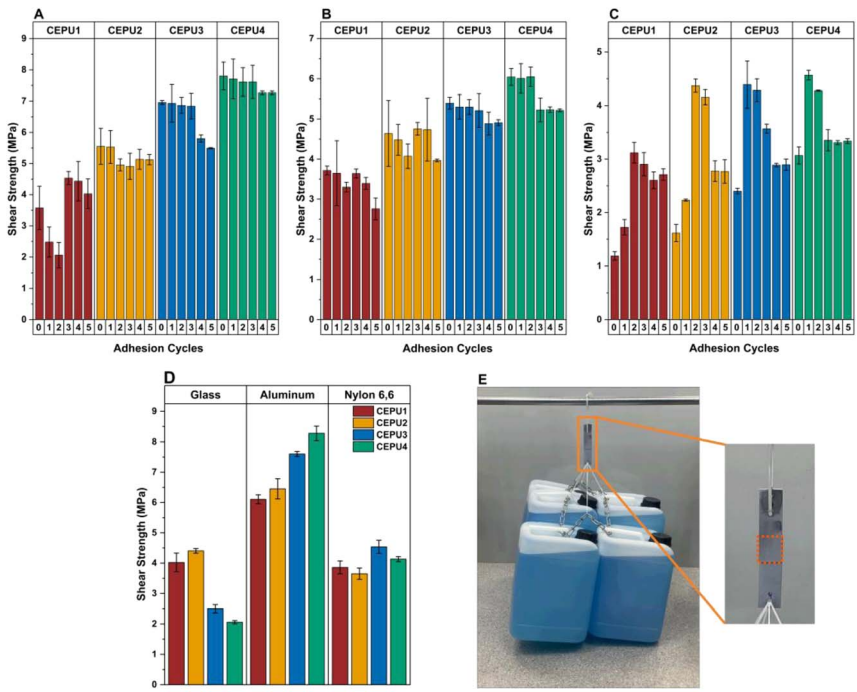

Fig. 5 Comparison of the shear strength of **CEPU1–CEPU4** over five re-adhesion cycles (30 min per cycle at 150 °C). Lap shear strength on (A) aluminium, (B) glass, and (C) Nylon 6,6. (D) Lap shear strength for one cycle after 2.5 hours at 150 °C. The error shown is the standard deviation between the three repeats for each sample. (E) Photograph of two aluminium plates bonded by **CEPU4** with 2.5 cm^2 bonding area (thickness ~200 μm) bearing six water containers weighing 120 kg.

three substrates. Generally, the CEPUs were observed to maintain or increase their shear strength over the five re-adhesion cycles, this was attributed to the increased wetting of the CEPUs on the substrate surface. To further illustrate the adhesive strength of the CEPUs, after five re-adhesion cycles 25 mg of **CEPU4** was re-adhered to the aluminium substrate from which 120 kg of water was suspended, see Fig. 5E. Adhering the CEPUs for 2.5 hours at 150 °C was used to show increased wetting of substrates was observed, see Fig. 5D and Table S4.† With exception of **CEPU3** and **CEPU4** on glass, the adhesive shear strength of the CEPUs after 2.5 hours was comparable to the shear strength after five re-adhesion cycles. Contrary to the re-adhesion cycles, after adhering for 2.5 hours on glass **CEPU3** and **CEPU4** observe significantly lower shear strengths and exhibited cohesive failure during testing.[47] FT-IR spectroscopic analysis of the CEPUs post adhesion revealed the νC═O stretching vibration at *ca.* 1700 cm^{-1}, see Fig. S15,† attributed to the urethanes in the polymer backbone, decreased in intensity with the emergence of a new absorbance band at 1642 cm^{-1} which could correspond to the formation of urea functionality within the bulk polymer.[48,49] Further comparisons between CEPUs *vs.* literature cross-linked debondable adhesives and debonding methods are made in Table S5.†

The inherent insolubility of the CEPUs, as a consequence of their crosslinked nature, hinders the ability to directly monitor the degradation of the CEPUs upon exposure to base. Therefore, to observe the base triggered degradation, 100 mg of CEPU was placed in THF (10 mL), aliquots of this solution were taken and

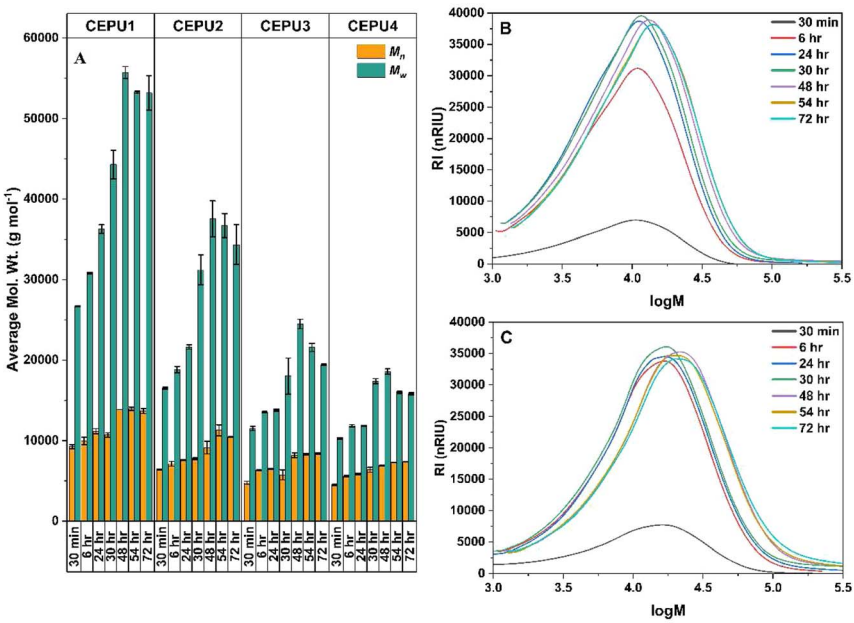

Fig. 6 (A) M_n and M_w of **CEPU1–CEPU4** after 30 minutes, 6, 24, 30, 48, 54, and 72 hours post addition of TBAF (1 M) acquired from a THF GPC; the recorded are averages of three separate samples of each CEPU. The error shown is the standard deviation between the three repeats of each sample. (B) GPC eluogram of **CEPU1** and (C) GPC eluogram of **CEPU4** in THF after 30 minutes, 6, 24, 30, 48, 54, and 72 hours post addition of TBAF (1 M).

analysed *via* GPC analysis, high or low molecular weight species were not evident after 24 hours. Upon the addition of 1 M TBAF in THF subsequent aliquots were taken and analysed *via* GPC analysis after 30 minutes, 6, 24, 30, 48, 54, and 72 hours, see Fig. 6, Fig. S16 and Table S6.† Two distinct trends are observed from the degradation analysis; the first shows as the molar ratio of the SDE is increased within the CEPU the molecular weight of the degraded polymer decreases, indicating the number of PTHF–HMDI repeat units in the polymer backbone decreases. The second trend shows the M_w of the solubilised degraded polymer material increases up to 48 hours post addition at which point narrowing of the molecular weight is observed, suggesting the depolymerization of the CEPUs facilitates the solubilisation of high molecular weight fragments which in turn undergo depolymerization themselves. This trend is reinforced by the full solubilisation of the CEPUs after 6 hours of exposure to TBAF.

Having established the capacity for the crosslinked CEPUs to degrade in the presence of base solutions, the debond-on-demand properties were tested upon exposure to 1 M $TBAF_{(aq)}$, with the best performing adhesive for each substrate, see Fig. 7 and Table S7.† We have previously shown with our linear CEPUs featuring the 2,2′-sulfonyldiethanol chain-extender, debonding of the adhesive could be achieved within 30 min of exposure to base solutions.[40] Therefore, all samples were exposed to base for 30 min, the debond-on-demand procedure for the adhered samples is outlined in the ESI.† The greatest loss in shear strength was observed with **CEPU4** when adhered to aluminium substrate of 34%, from 7.71 MPa to 5.11 MPa.

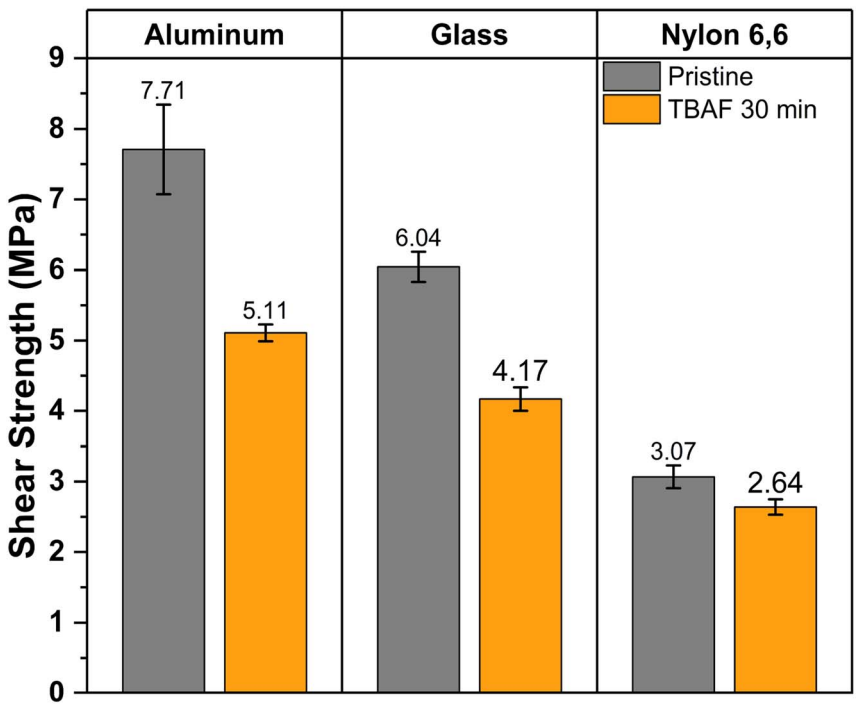

Fig. 7 Shear strength of **CEPU4** on aluminium, glass, and Nylon 6,6 after exposure to 1 M $TBAF_{(aq)}$ for 30 minutes.

Conclusions

To meet current industrial and commercial needs for strongly adhering and rapidly degradable crosslinked polyurethanes, a series of base triggered depolymerisable CEPUs featuring the commercially available 2,2′-sulfonyldiethanol chain-extender have been generated for use as 'debond-on-demand' adhesives. Variations in the CEPU composition, *i.e.* increasing the hard segment content, facilitated the tailoring of the mechanical, adhesive, and depolymerisable characteristics of the CEPUs. Increases in the CEPU hard content resulted in significant increases in the mechanical properties, with **CEPU4** exhibiting an ultimate tensile strength of 42.68 MPa and elongation at break of 17.59 ε. **CEPU4**, derived from entirely commercially available materials, was shown to have comparable adhesive characteristics to those described within the literature when adhered to a range of substrates. Upon exposure to TBAF, depolymerization of the crosslinked CEPUs occurs characterized by the generation of a range of low molecular weight species and the solubilization of the previously insoluble polymer. Investigation of the base triggered 'debond-on-demand' characteristics of **CEPU4** revealed losses in shear strength of 34% (aluminium substrate) could be achieved, from 7.71 MPa to 5.11 MPa, after only 30 minutes exposure to 1 M $TBAF_{(aq)}$.

Data availability

The data supporting this article have been included as part of the ESI.†

Author contributions

Alarqam Z. Tareq: conceptualisation, validation, formal analysis, investigation, writing – original draft. Matthew Hyder: conceptualisation, formal analysis, investigation, visualization, writing – original draft. Josephine L. Harries: supervision & editing. Wayne Hayes: conceptualisation, resources, writing – review & editing, supervision, project administration. All authors reviewed the manuscript.

Conflicts of interest

There are no conflicts to declare.

Acknowledgements

The authors would like to acknowledge the financial support from HCED Iraq (PhD studentship for A. Z. T.) and from the University of Reading and Domino Printing Sciences Ltd (PhD studentship for M. H.). In addition, the University of Reading (EPSRC – Doctoral Training Grant) is acknowledged for providing access to instrumentation in the Chemical Analysis Facility. We thank Mr Nick Spencer (Chemical Analysis Facility (CAF), University of Reading) for collecting the SAXS and WAXS data.

References

1 T. Türel, A. M. Cristadoro, M. Linnenbrink and Ž. Tomović, *ACS Appl. Mater. Interfaces*, 2025, **17**, 2656–2665.
2 S. J. Knight, J. D. McCoy, S. Chowdhury and Y. Lee, *Polym. Test.*, 2025, **146**, 108776.
3 A. Z. Tareq, M. Hyder, D. H. Merino, A. M. Chippindale, A. Kaur, J. A. Cooper and W. Hayes, *Polymer*, 2024, **302**, 127052.
4 D. K. Chattopadhyay and K. V. S. N. Raju, *Prog. Polym. Sci.*, 2007, **32**, 352–418.
5 A. D. O'Donnell, M. Hyder, A. M. Chippindale, J. L. Harries, I. M. German and W. Hayes, *ACS Appl. Polym. Mater.*, 2024, **6**, 15242–15252.
6 S. Xinrong, W. Nanfang, S. Kunyang, D. Sha and C. Zhen, *J. Ind. Eng. Chem.*, 2014, **20**, 3228–3233.
7 M. Vaishali, S. Gopal and K. J. Sreeram, *RSC Sustainability*, 2024, **2**, 2324–2334.
8 T. Griggs, J. Ahmed, H. Majd, M. Edirisinghe and B. Chen, *Mater. Adv.*, 2024, **5**, 6210–6221.
9 W. Zhang, M. Ren, M. Chen and L. Wu, *RSC Adv.*, 2025, **15**, 6231–6240.
10 G. Kaur, R. Adhikari, P. Cass, M. Bown, M. D. M. Evans, A. V. Vashi and P. Gunatillake, *RSC Adv.*, 2015, **5**, 98762–98772.
11 B. Liu, Z. Liu, H. Wei, Y. Meng, Q. Hou, A. Wang, Y. Zhang, E. Han, S. Hu and J. Zhou, *RSC Adv.*, 2024, **14**, 10858–10873.
12 E. B. Iezzi, G. C. Daniels, K. Sutyak and E. Camerino, *ACS Appl. Polym. Mater.*, 2024, **6**, 8178–8190.
13 Y. Zhou, L. Zhu, J. Zhai, R. Yang and X. Guo, *Polymer*, 2023, **285**, 126356.
14 N. D. Blelloch, H. J. Yarbrough and K. A. Mirica, *Chem. Sci.*, 2021, **12**, 15183–15205.
15 H. Mutlu, C. M. Geiselhart and C. Barner-Kowollik, *Mater. Horiz.*, 2018, **5**, 162–183.
16 J. Gong, B. Tavsanli and E. R. Gillies, *Annu. Rev. Mater. Res.*, 2024, **54**, 47–73.
17 A. G. Gavriel, M. R. Sambrook, A. T. Russell and W. Hayes, *Polym. Chem.*, 2022, **13**, 3188–3269.
18 A. del Prado, D. K. Hohl, S. Balog, L. M. de Espinosa and C. Weder, *ACS Appl. Polym. Mater.*, 2019, **1**, 1399–1409.
19 C. Heinzmann, S. Coulibaly, A. Roulin, G. L. Fiore and C. Weder, *ACS Appl. Mater. Interfaces*, 2014, **6**, 4713–4719.
20 C. Heinzmann, U. Salz, N. Moszner, G. L. Fiore and C. Weder, *ACS Appl. Mater. Interfaces*, 2015, **7**, 13395–13404.
21 S. Salimi, T. S. Babra, G. S. Dines, S. W. Baskerville, W. Hayes and B. W. Greenland, *Eur. Polym. J.*, 2019, **121**, 109264.
22 C. Heinzmann, I. Lamparth, K. Rist, N. Moszner, G. L. Fiore and C. Weder, *Macromolecules*, 2015, **48**, 8128–8136.
23 W. Denissen, J. M. Winne and F. E. Du Prez, *Chem. Sci.*, 2016, **7**, 30–38.
24 F. Van Lijsebetten, K. De Bruycker, E. Van Ruymbeke, J. M. Winne and F. E. Du Prez, *Chem. Sci.*, 2022, **13**, 12865–12875.
25 A. J. Inglis, L. Nebhani, O. Altintas, F. G. Schmidt and C. Barner-Kowollik, *Macromolecules*, 2010, **43**, 5515–5520.
26 M. Inada, T. Horii, T. Fujie, T. Nakanishi, T. Asahi and K. Saito, *Mater. Adv.*, 2023, **4**, 1289–1296.

27 J. Liu, A. Pich and K. V. Bernaerts, *Green Chem.*, 2024, **26**, 1414–1429.
28 X. Huang, C. Ding, Y. Wang, S. Zhang, X. Duan and H. Ji, *ACS Appl. Mater. Interfaces*, 2024, **16**, 38586–38605.
29 T. S. Babra, A. Trivedi, C. N. Warriner, N. Bazin, D. Castiglione, C. Sivour, W. Hayes and B. W. Greenland, *Polym. Chem.*, 2017, **8**, 7207–7216.
30 Y. Oh, J. Park, J.-J. Park, S. Jeong and H. Kim, *Chem. Mater.*, 2020, **32**, 6384–6391.
31 P. Damacet, H. J. Yarbrough, N. D. Blelloch, H.-J. Noh and K. A. Mirica, *Polym. Chem.*, 2024, **15**, 1112–1122.
32 S. H. Jung, G. Choi, S. Jeong, J. Park, H. Yoon, J.-J. Park and H. Kim, *ACS Sustainable Chem. Eng.*, 2022, **10**, 13816–13824.
33 T. S. Babra, M. Wood, J. S. Godleman, S. Salimi, C. Warriner, N. Bazin, C. R. Siviour, I. W. Hamley, W. Hayes and B. W. Greenland, *Eur. Polym. J.*, 2019, **119**, 260–271.
34 T. S. Babra, C. Warriner, N. Bazin, W. Hayes and B. W. Greenland, *Mater. Today Commun.*, 2021, **26**, 101777.
35 K. B. Sutyak, E. B. Iezzi, G. C. Daniels and E. Camerino, *ACS Appl. Mater. Interfaces*, 2022, **14**, 22407–22417.
36 G. C. Daniels, E. Camerino, J. H. Wynne and E. B. Iezzi, *Mater. Horiz.*, 2018, **5**, 831–836.
37 J. Han, Y. Zhou, G. Bai, W. Wei, X. Liu and X. Li, *Mater. Chem. Front.*, 2022, **6**, 503–511.
38 J. Han, M. Dai, G. Bai, M. Wei, J. Liu, W. Wei, X. Liu and X. Li, *Eur. Polym. J.*, 2023, **195**, 112210.
39 J. Han, S. Li, W. Zhang, M. Wei, J. Liu, W. Wei, X. Liu and X. Li, *ACS Appl. Polym. Mater.*, 2024, **6**, 712–721.
40 M. J. Hyder, J. Godleman, A. M. Chippindale, J. E. Hallett, T. Zinn, J. L. Harries and W. Hayes, *Macromolecules*, 2025, **58**, 681–696.
41 C. Fodor, A. Domján and B. Iván, *Polym. Chem.*, 2013, **4**, 3714–3724.
42 K. N. Raftopoulos, B. Janowski, L. Apekis, K. Pielichowski and P. Pissis, *Eur. Polym. J.*, 2011, **47**, 2120–2133.
43 P. J. Woodward, D. Hermida Merino, B. W. Greenland, I. W. Hamley, Z. Light, A. T. Slark and W. Hayes, *Macromolecules*, 2010, **43**, 2512–2517.
44 D. H. Merino, A. Feula, K. Melia, A. T. Slark, I. Giannakopoulos, C. R. Siviour, C. P. Buckley, B. W. Greenland, D. Liu, Y. Gan, P. J. Harris, A. M. Chippindale, I. W. Hamley and W. Hayes, *Polymer*, 2016, **107**, 368–378.
45 A. Z. Tareq, M. Hyder, D. H. Merino, S. D. Mohan, J. A. Cooper and W. Hayes, *Eur. Polym. J.*, 2025, **228**, 113782.
46 X. Li, W. Xu, W. Yuan, K. Liu, J. Zhou, G. Shan, Y. Bao and P. Pan, *Polymer*, 2021, **222**, 123670.
47 J. Tang, L. Wan, Y. Zhou, H. Pan and F. Huang, *J. Mater. Chem. A*, 2017, **5**, 21169–21177.
48 F. Xie, T. Zhang, P. Bryant, V. Kurusingal, J. M. Colwell and B. Laycock, *Prog. Polym. Sci.*, 2019, **90**, 211–268.
49 Z. Ying, C. Wu, S. Jiang, R. Shi, B. Zhang, C. Zhang and F. Zhao, *Green Chem.*, 2016, **18**, 3614–3619.